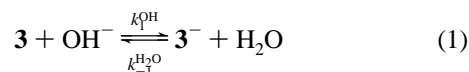


**Figure 1.** Time-dependent absorption spectra for the deprotonation of  $7.5 \times 10^{-5}$  M **3** by 0.14 M Me<sub>4</sub>NOH in 50% MeCN–50% water. Spectra taken at 16-ms intervals.

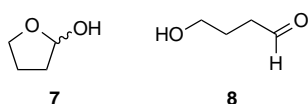
## Results

**General Features.** The reaction of **3** with KOH or Me<sub>4</sub>NOH in 50% MeCN–50% water (v/v) is characterized by two distinct kinetic processes at [KOH]  $\geq$  0.01 M or [Me<sub>4</sub>NOH]  $\geq$  0.005 M. The first is in the subsecond range and can be attributed to the reversible deprotonation of **3** described by eq 1. Figure 1 shows the spectral changes associated with this

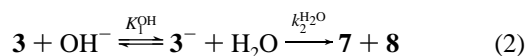


process as measured in a stopped-flow spectrophotometer. The specific example displayed in the figure refers to a Me<sub>4</sub>NOH solution because more of the anion **3**<sup>−</sup> is formed in such a solution than in a KOH/MeCN/H<sub>2</sub>O solution (more on this below), leading to a larger spectral change.

The second process is well separated from the first and occurs in a time frame of seconds; it leads to irreversible hydrolytic decomposition of **3**<sup>−</sup> to form the hemiacetal 2-hydroxytetrahydrofuran (**7**) in equilibrium with a small amount of its acyclic



form, 4-hydroxybutanal (**8**). Assuming that this decomposition occurs by the same mechanism as that for the irreversible decomposition of the conjugate anions of **2a**, **2b**, and **6** under similar conditions,<sup>12,13</sup> it can be represented as a reaction of **3**<sup>−</sup> with water, as indicated by eq 2 where the proton transfer



represents a fast preequilibrium. The validity of this mechanism has been scrutinized elsewhere.<sup>14</sup> Hence in the present paper kinetic data for this process will only be reported to the extent that they are necessary for the interpretation of the results for the proton transfer (see under Kinetic Isotope Effects).

All kinetic data were obtained under pseudo-first-order conditions with the carbene complex as the minor component.

(12) Bernasconi, C. F.; Flores, F. X.; Sun, W. *J. Am. Chem. Soc.* **1995**, *117*, 4875.

(13) Bernasconi, C. F.; Sun, W. *Organometallics* **1995**, *14*, 5615.

(14) Bernasconi, C. F.; Leyes, A. E. *J. Chem. Soc., Perkin Trans. 2* In press.

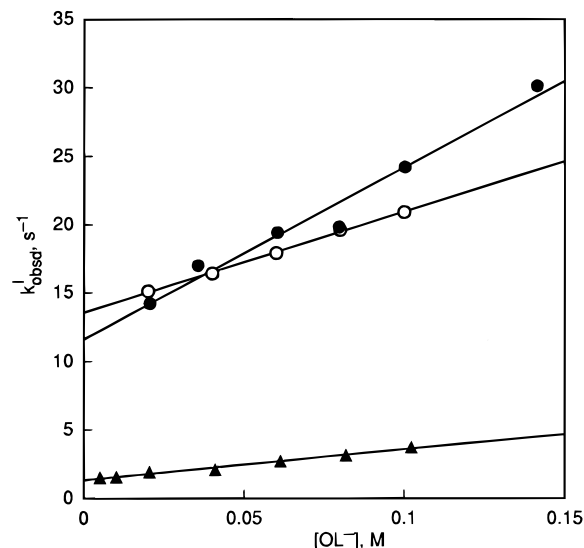


**Figure 2.** Plots of  $k_{\text{obsd}}^{\text{I}}$  vs  $[\text{OL}^-]$  for proton transfer. (O) Reaction with KOH in 50% MeCN–50% H<sub>2</sub>O; (●) reaction with Me<sub>4</sub>NOH in 50% MeCN–50% H<sub>2</sub>O; (▲) reaction with KOD in 50% MeCN–50% D<sub>2</sub>O.

The pseudo-first-order rate constants for the fast process (proton transfer) will be denoted as  $k_{\text{obsd}}^{\text{I}}$ , that for the slow process (hydrolysis of **3**<sup>−</sup>) as  $k_{\text{obsd}}^{\text{II}}$ . Unless stated otherwise, the ionic strength was maintained at 0.1 M with KCl, or Me<sub>4</sub>NCl in the experiments with Me<sub>4</sub>NOH as the base.

**Reaction of **3** with KOH and Me<sub>4</sub>NOH.** Pseudo-first-order rate constants ( $k_{\text{obsd}}^{\text{I}}$ ) were measured in KOH (0.02 to 0.1 M) and Me<sub>4</sub>NOH (0.02 to 0.14 M)<sup>15</sup> solutions. The raw data are summarized elsewhere.<sup>16</sup> Plots of  $k_{\text{obsd}}^{\text{I}}$  vs [KOH] and [Me<sub>4</sub>NOH] are shown in Figure 2. They are consistent with reversible deprotonation of **3** for which  $k_{\text{obsd}}^{\text{I}}$  is given by eq 3.

$$k_{\text{obsd}}^{\text{I}} = k_1^{\text{OH}}[\text{OH}^-] + k_{-1}^{\text{H}_2\text{O}} \quad (3)$$

For the KOH reactions, one obtains  $k_1^{\text{OH}} = 74 \pm 2 \text{ M}^{-1} \text{ s}^{-1}$  from the slope and  $k_{-1}^{\text{H}_2\text{O}} = 14 \pm 1 \text{ s}^{-1}$  from the intercept; this yields an equilibrium constant  $K_1^{\text{OH}} = k_1^{\text{OH}}/k_{-1}^{\text{H}_2\text{O}} = 5.29 \pm 0.55 \text{ M}^{-1}$  or  $\text{p}K_{\text{a}}^{\text{CH}} = 14.47 \pm 0.04$  based on  $\text{p}K_{\text{w}} = 15.19$  in 50% MeCN–50% water.<sup>10</sup> For the Me<sub>4</sub>NOH reaction,  $k_1^{\text{OH}} = 128 \pm 6 \text{ M}^{-1} \text{ s}^{-1}$ ,  $k_{-1}^{\text{H}_2\text{O}} = 11.6 \pm 0.6 \text{ s}^{-1}$ , and  $K_1^{\text{OH}} = 11.03 \pm 1.15 \text{ M}^{-1}$ ; no  $\text{p}K_{\text{a}}^{\text{CH}}$  is calculated from  $K_1^{\text{OH}}$  because  $\text{p}K_{\text{w}}$  in the presence of Me<sub>4</sub>N<sup>+</sup> as counter ion is not known.

Because  $\text{p}K_{\text{a}}^{\text{CH}}$  is not much lower than  $\text{p}K_{\text{w}}$ , deprotonation of **3** is far from complete even at the higher base concentrations used, especially in KOH solutions where the  $[\mathbf{3}^-]/[\mathbf{3}]$  ratio at the highest [KOH] of 0.1 M is only  $K_1^{\text{OH}}[\text{OH}^-] = 0.53$ . This explains the relatively weak dependence of  $k_{\text{obsd}}$  on base concentration (Figure 2) and also the relatively small absorption changes ( $\Delta\text{OD}$ ) observed during the reaction. The use of higher [KOH] was precluded by solubility limitations.

With Me<sub>4</sub>NOH, the somewhat higher  $K_1^{\text{OH}}$  value and the slightly higher solubility leads to a  $[\mathbf{3}^-]/[\mathbf{3}]$  ratio of 1.60 at the highest [Me<sub>4</sub>NOH] of 0.14 M. This means that for the Me<sub>4</sub>NOH reaction the range of the  $[\mathbf{3}^-]/[\mathbf{3}]$  ratio at various base concentrations was wide enough to allow determination of an approximate value of  $K_1^{\text{OH}}$  based on the dependence of the  $\Delta\text{OD}$  values on Me<sub>4</sub>NOH concentration. This dependence is

(15) At the highest Me<sub>4</sub>NOH concentrations the ionic strength was higher than 0.1 M.

(16) Leyes, A. E. Doctoral Thesis, University of California, Santa Cruz, 1996.

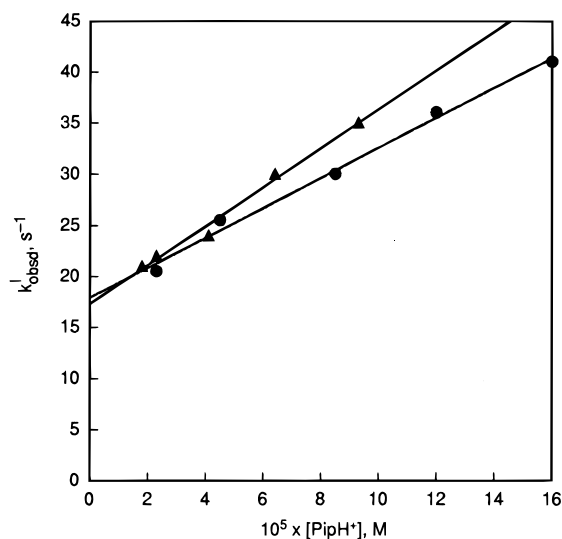


**Figure 3.** Plots of  $k_{\text{obsd}}^1$  vs piperidinium ion concentration; ● and ▲ represent two different series of runs, see text.

given by eq 4 where  $\Delta\text{OD}_0$  is the change in absorbance if

$$\frac{1}{\Delta\text{OD}} = \frac{1}{\Delta\text{OD}_0} + \frac{1}{\Delta\text{OD}_0 \cdot K_1^{\text{OH}}[\text{OH}^-]} \quad (4)$$

conversion of **3** to **3<sup>-</sup>** were complete. A plot of  $\Delta\text{OD}^{-1}$  vs  $[\text{OH}^-]^{-1}$  (not shown) yields  $\Delta\text{OD}_0 = 0.63 \pm 0.16$  and  $K_1^{\text{OH}} = 6.3 \pm 2.1 \text{ M}^{-1}$ . Considering the large uncertainty in the  $\Delta\text{OD}$  values obtained from stopped-flow traces, the agreement with the kinetic  $K_1^{\text{OH}}$  value of  $11.03 \text{ M}^{-1}$  is remarkably good. More importantly, the adherence of  $\Delta\text{OD}$  to eq 4 constitutes corroborating evidence that the observed process is an equilibrium reaction and indeed corresponds to proton transfer.

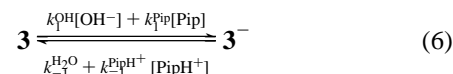
**Reaction of **3<sup>-</sup>** with Piperidinium Ion.** The reversibility of the proton transfer was further demonstrated by reacting **3<sup>-</sup>** with piperidinium ion, which led to nearly quantitative recovery of **3**. In these experiments, **3<sup>-</sup>** was transiently generated by reacting **3** with 0.1 M KOH in the pre-mixing chamber of a double-mixing stopped-flow apparatus. After about 300 ms, the solution containing **3<sup>-</sup>** was mixed with a piperidine buffer containing enough acid to neutralize most of the KOH and yield a final pH of 13.85. This pH was chosen to keep the piperidinium ion concentration low enough ( $\text{p}K_{\text{a}}^{\text{PipH}^+} = 11.01$ )<sup>10</sup> that the rate of protonation of **3<sup>-</sup>** by piperidinium ion is not too fast for the stopped-flow method, and at the same time to keep the  $\text{OH}^-$  concentration high enough to ensure good buffering of the solution.

The results of the rate determinations are shown in Figure 3. Two series of runs were carried out under similar conditions. The slope from the first series was  $(1.5 \pm 0.1) \times 10^5 \text{ M}^{-1} \text{ s}^{-1}$ , that for the second series  $(1.9 \pm 0.1) \times 10^5 \text{ M}^{-1} \text{ s}^{-1}$ ; we shall use the average of  $1.7 \times 10^5 \text{ M}^{-1} \text{ s}^{-1}$  in our further discussions. The intercepts from the two series,  $17 \pm 1$  and  $17.3 \pm 0.6 \text{ s}^{-1}$ , were indistinguishable.

The expression for  $k_{\text{obsd}}$  in the piperidine buffers is given by eq 5, reflecting the expansion of the reaction scheme of eq 1 to

$$\begin{aligned} k_{\text{obsd}}^1 &= k_1^{\text{OH}}[\text{OH}^-] + k_{-1}^{\text{H}_2\text{O}} + k_1^{\text{Pip}}[\text{Pip}] + k_{-1}^{\text{PipH}^+}[\text{PipH}^+] \\ &= k_1^{\text{OH}}[\text{OH}^-] + k_{-1}^{\text{H}_2\text{O}} + k_{-1}^{\text{PipH}^+} \left( 1 + \frac{K_{\text{a}}^{\text{CH}}}{a_{\text{H}^+}} \right) [\text{PipH}^+] \end{aligned} \quad (5)$$

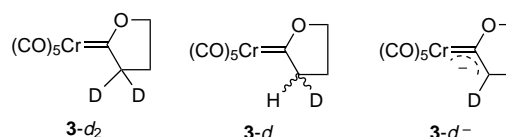
that of eq 6. The slope in Figure 3 can be equated with



$k_{-1}^{\text{PipH}^+}(1 + K_{\text{a}}^{\text{CH}}/a_{\text{H}^+})$ , which affords  $k_{-1}^{\text{PipH}^+} = (1.36 \pm 0.30) \times 10^5 \text{ M}^{-1} \text{ s}^{-1}$ ; from this  $k_{-1}^{\text{PipH}^+}$  value one can also calculate  $k_1^{\text{Pip}} = 47 \pm 12 \text{ M}^{-1} \text{ s}^{-1}$ . The intercept (average  $17.2 \text{ s}^{-1}$ ) is in excellent agreement with the expected value ( $17.4 \text{ s}^{-1}$ ) based on  $k_1^{\text{OH}} = 74 \text{ M}^{-1} \text{ s}^{-1}$  and  $k_{-1}^{\text{H}_2\text{O}} = 14 \text{ s}^{-1}$  determined in the KOH experiments. All proton transfer rate constants are summarized in Table 1.

**Kinetic Isotope Effects.** Three types of kinetic isotope effect experiments for proton transfer and hydrolysis were performed.

**(1) Reactions of **3-d<sub>2</sub>** with KOD in 50% MeCN–50% D<sub>2</sub>O:**



The interpretation of the results of these reactions is simple because the scheme of eq 1 can be applied, except that all active protons have been substituted by deuterons. In the range of 0.005 to 0.1 M KOD, both deuteron transfer and hydrolytic decomposition of **3<sup>-</sup>** can be observed as two distinct and well-separated kinetic processes. A plot of  $k_{\text{obsd}}^1$  vs  $[\text{KOD}]$  for the deuteron transfer is included in Figure 2. It yields  $k_{1,\text{D}}^{\text{OD}} = 22.2 \pm 1.2 \text{ M}^{-1} \text{ s}^{-1}$ ,  $k_{-1,\text{D}}^{\text{D}_2\text{O}} = 1.33 \pm 0.07 \text{ s}^{-1}$ , and  $K_{1,\text{D}}^{\text{OD}} = 16.7 \pm 1.8 \text{ M}^{-1}$ .<sup>17</sup>

**(2) Reactions of **3** with KOD in 50% MeCN–50% D<sub>2</sub>O:**

These reactions are complex and characterized by three kinetic processes, as shown in Figure 4. As discussed in more detail below, this kinetic behavior can be rationalized as arising from deprotonation of **3** by  $\text{OD}^-$  (first process), followed by trapping of **3<sup>-</sup>** by  $\text{D}_2\text{O}$  to yield **3-d** and **3-d<sub>2</sub>** (partial recovery of absorbance at 364 nm), and subsequent hydrolysis (final decay). In analyzing the kinetic traces we could only determine reliable pseudo-first-order rate constants for the first and third process. This was done at six KOD concentrations between 0.005 and 0.1 M. The results are summarized in Table 2.

No attempts were made to directly extract rate constants for proton/deuteron transfer or hydrolysis from these data because of the complex nature of the various processes involving simultaneous dehydronation<sup>18</sup> of **3**, **3-d**, **3-d<sub>2</sub>**, and deuteration of **3<sup>-</sup>** and **3-d<sup>-</sup>** by  $\text{D}_2\text{O}$ . Instead, computer simulations were performed on the basis of Scheme 1 ( $\text{CH}_2 = \mathbf{3}$ ,  $\text{CH} = \mathbf{3}^-$ ,  $\text{CHD} = \mathbf{3-d}$ ,  $\text{CD} = \mathbf{3-d}^-$ ,  $\text{CD}_2 = \mathbf{3-d}_2$ ) and known or estimated rate constants for the various steps in Scheme 1 which would reproduce the triphasic kinetic traces such as shown in Figure 4. Of the eight rate constants in Scheme 1, three were known from the experiments with **3-d<sub>2</sub>** in KOD solutions:  $k_{1,\text{D}}^{\text{OD}}$ ,  $k_{-1,\text{D}}^{\text{D}_2\text{O}}$ , and  $k_{2,\text{D}}^{\text{D}_2\text{O}}$ .<sup>20</sup> Assuming negligible secondary isotope effects<sup>21</sup> allowed us to set  $k_{-1,\text{H}}^{\text{D}_2\text{O}} = k_{-1,\text{D}}^{\text{D}_2\text{O}}$ ,  $k_{1,\text{HD}}^{\text{OD}} = 1/2 k_{1,\text{D}}^{\text{OD}}$ ,<sup>23</sup>  $k_{1,\text{HD}}^{\text{OD}} = 1/2 k_{1,\text{D}}^{\text{OD}}$ ,<sup>23</sup> and  $k_{2,\text{H}}^{\text{D}_2\text{O}} = k_{2,\text{D}}^{\text{D}_2\text{O}}$ . This leaves  $k_{1,\text{H}}^{\text{OH}}$  as the only

(17) The subscripts H and D refer to the substrate (**3** vs **3-d<sub>2</sub>**, **3<sup>-</sup>** vs **3-d<sup>-</sup>**).  $K_{1,\text{H}}^{\text{OH}}$  is identical to  $K_{1,\text{H}}^{\text{OH}}$  and  $k_{-1,\text{H}}^{\text{H}_2\text{O}}$  is identical to  $k_{-1,\text{H}}^{\text{H}_2\text{O}}$  used in eq 5.

(18) Hydron refers to either proton or deuterium and is the name recommended by the IUPAC Commission on Physical Organic Chemistry.<sup>19</sup>

(19) Bunnett, J. F.; Jones, R. A. Y. *Pure Appl. Chem.* **1988**, *60*, 1115.

(20)  $k_{2,\text{D}}^{\text{D}_2\text{O}}$  from ref 14.

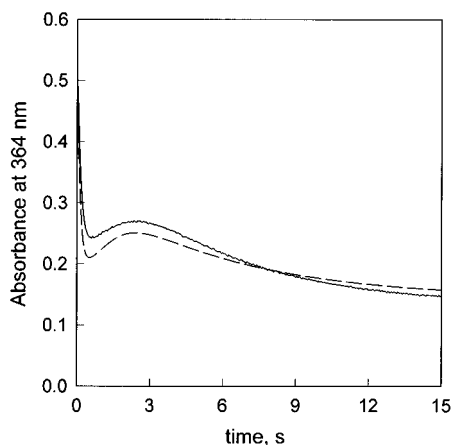
(21) Secondary isotope effects may arise because deprotonation induces a change in hybridization of the  $\alpha$ -carbon from  $\text{sp}^3$  to  $\text{sp}^2$ . Such secondary isotope effects are typically quite small.<sup>22</sup>

(22) (a) Melander, L.; Saunders, W. J., Jr. *Reaction Rates of Isotopic Molecules*; Wiley-Interscience: New York, 1980; p 170. (b) Bell, R. P. *The Proton in Chemistry*; Cornell University Press: Ithaca, New York, 1973; p 260.

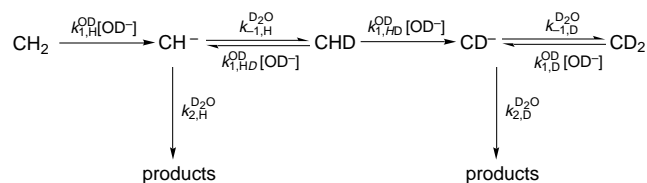
**Table 1.** Summary of Proton Transfer Rate Constants in 50% MeCN–50% Water at 25 °C

parameter	<b>3</b>	<b>2a<sup>a</sup></b>	<b>6<sup>a</sup></b>
$\text{p}K_{\text{a}}^{\text{CH}}$	$14.47 \pm 0.04^{b,c}$ (14.77) <sup>d</sup>	12.50 (12.98) <sup>d</sup>	10.40 (10.70) <sup>d</sup>
$k_{-1}^{\text{OH}}, \text{M}^{-1} \text{s}^{-1}$	$74 \pm 2$ (37) <sup>d</sup>	456 (152) <sup>d</sup>	115 (57.5) <sup>d</sup>
$k_{-1}^{\text{H}_2\text{O}}, \text{s}^{-1}$	$14 \pm 1$	0.91	0.0019
$K_{-1}^{\text{OH}}, \text{M}^{-1}$	$5.29 \pm 0.55$ (2.64) <sup>d</sup>	501 (167) <sup>d</sup>	$6.05 \times 10^4$ ( $3.03 \times 10^4$ ) <sup>d</sup>
$k_{-1}^{\text{Pip}}, \text{M}^{-1} \text{s}^{-1}$	$47 \pm 12$ (23.5) <sup>d</sup>	906 (302) <sup>d</sup>	225 (112) <sup>d</sup>
$k_{-1}^{\text{PipH}^+}, \text{M}^{-1} \text{s}^{-1}$	$(1.36 \pm 0.30) \times 10^5$	$2.77 \times 10^4$	55
$\log k_{\text{o}}^{\text{OH}^e}$	1.51 (1.36) <sup>d</sup>	1.31 (1.07) <sup>d</sup>	-0.33 (-0.48) <sup>d</sup>
$\log k_{\text{o}}^{\text{R}_2\text{NH}^e}$	3.51 (3.40) <sup>d</sup>	3.62 (3.37) <sup>d</sup>	1.80 (1.69) <sup>d,f</sup>

<sup>a</sup> Reference 10. <sup>b</sup> Determined with KOH; the values for **3** with Me<sub>3</sub>NOH are  $k_{-1}^{\text{OH}} = 128 \pm 6 \text{ M}^{-1} \text{ s}^{-1}$ ,  $k_{-1}^{\text{H}_2\text{O}} = 11.6 \pm 0.6 \text{ s}^{-1}$ , and  $K_{-1}^{\text{OH}} = 11.03 \pm 1.15$ . <sup>c</sup>  $\text{p}K_{\text{a}}^{\text{CH}} = \text{p}K_{\text{w}} - \log K_{-1}^{\text{OH}}$ , with  $\text{p}K_{\text{w}} = 15.19$  (ref 10). <sup>d</sup> Statistically corrected for number of equivalent acidic protons. <sup>e</sup> Obtained as described in the text. <sup>f</sup>  $\beta = 0.48$  in this case (ref 10).

**Figure 4.** Reaction of  $7.4 \times 10^{-5} \text{ M}$  **3** with 0.041 M KOD in 50% MeCN–50% D<sub>2</sub>O: (—): experimental kinetic trace at 364 nm; (---) simulated trace as described in text.**Table 2.** Experimental and Simulated  $k_{\text{obsd}}$  Values for the Reaction of **3** with KOD in 50% MeCN–50% D<sub>2</sub>O

[KOD], M	$k_{\text{obsd}}^{\text{I}}, \text{s}^{-1}$		$k_{\text{obsd}}^{\text{II}}, \text{s}^{-1}$	
	exptl	simulated	exptl	simulated
0.0051	1.78	1.92	0.0136	0.040
0.0205	3.96	4.11	0.097	0.119
0.0410	6.64	6.70	0.195	0.196
0.0614	9.53	9.41	0.255	0.253
0.1023	18.9	14.5	0.405	0.326

**Scheme 1**

unknown. The simulations were performed by starting with an initial estimate of  $k_{1,\text{H}}^{\text{OD}^-} = 1.5k_{1,\text{H}}^{\text{OH}^-}$  and then using several iterations to find the value that would give the best fit with the experimental traces at the various KOD concentrations. A comparison between an experimental and simulated curve is shown in Figure 4. In view of the various approximations made, the fit between the two curves is reasonably good.

The various rate constants of Scheme 1 which provided the best fit are summarized in Table 3 along with the rate constants of the reactions of **3** with KOH and of **3-d<sub>2</sub>** with KOD. The computer simulation was also used to determine  $k_{\text{obsd}}^{\text{I}}$  and

(23) The factor  $1/2$  takes into account that CHD has only one proton and only one deuterium.

**Table 3.** Summary of Microscopic Rate Constants Obtained from Isotope Effect Experiments<sup>a</sup>

rate constant	kinetic isotope effect
$k_{1,\text{H}}^{\text{OH}} (\text{M}^{-1} \text{s}^{-1})^b$	$k_{1,\text{H}}^{\text{OH}}/k_{1,\text{D}}^{\text{OH}}$ 7.2
$k_{1,\text{D}}^{\text{OH}} (\text{M}^{-1} \text{s}^{-1})$	
$k_{1,\text{H}}^{\text{OD}} (\text{M}^{-1} \text{s}^{-1})$	$k_{1,\text{H}}^{\text{OD}}/k_{1,\text{D}}^{\text{OD}}$ 7.2
$k_{1,\text{D}}^{\text{OD}} (\text{M}^{-1} \text{s}^{-1})$	$22.2 \pm 1.2^c$
$k_{1,\text{H},\text{D}}^{\text{OD}} (\text{M}^{-1} \text{s}^{-1})$	$k_{1,\text{H},\text{D}}^{\text{OD}}/k_{1,\text{H},\text{D}}^{\text{OD}}$ 7.2
$k_{1,\text{H},\text{D}}^{\text{OD}} (\text{M}^{-1} \text{s}^{-1})$	
$k_{1,\text{H},\text{D}}^{\text{OD}} (\text{M}^{-1} \text{s}^{-1})$	$11.1^g$
$k_{-1,\text{H}}^{\text{H}_2\text{O}} (\text{s}^{-1})^h$	$k_{-1,\text{H}}^{\text{H}_2\text{O}}/k_{-1,\text{H}}^{\text{D}_2\text{O}}$ 10.5
$k_{-1,\text{H}}^{\text{D}_2\text{O}} (\text{s}^{-1})^j$	$1.33 \pm 0.07^j$

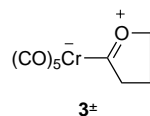
<sup>a</sup> Superscripts indicate base (OH<sup>-</sup> or OD<sup>-</sup>) or acid (H<sub>2</sub>O or D<sub>2</sub>O) while subscripts (H or D) refer to the hydron removed from the substrate or that on its conjugate anion, see, e.g., Scheme 1. <sup>b</sup>  $k_{1,\text{H}}^{\text{OH}}$  is the same as  $k_{1,\text{H}}^{\text{OH}}$  in eq 1. <sup>c</sup> Experimentally determined. <sup>d</sup> From  $k_{1,\text{H}}^{\text{OH}}/k_{1,\text{D}}^{\text{OH}} = k_{1,\text{H}}^{\text{OD}}/k_{1,\text{D}}^{\text{OD}}$ . <sup>e</sup> From computer simulation. <sup>f</sup> Assumed to be  $1/2k_{1,\text{H},\text{D}}^{\text{OD}}$ , see text. <sup>g</sup> Assumed to be  $1/2k_{1,\text{H},\text{D}}^{\text{OD}}$ , see text. <sup>h</sup>  $k_{-1,\text{H}}^{\text{H}_2\text{O}}$  is the same as  $k_{-1,\text{H}}^{\text{H}_2\text{O}}$  in eq 1. <sup>i</sup> Assumed to be the same as  $k_{-1,\text{D}}^{\text{D}_2\text{O}}$ . <sup>j</sup> Experimental value for  $k_{-1,\text{D}}^{\text{D}_2\text{O}}$ .

$k_{\text{obsd}}^{\text{II}}$  on the basis of the simulated traces. They are included in Table 2. The match between simulated and experimental rate constants is remarkably good except for  $k_{\text{obsd}}^{\text{II}}$  at the lowest [KOD]. The fact that the  $k_{2,\text{D}}^{\text{D}_2\text{O}}$  value (ca.  $0.37 \text{ s}^{-1}$ )<sup>20</sup> is quite close to the inherently more accurate  $k_{2,\text{D}}^{\text{D}_2\text{O}}$  value obtained from the reaction of **3-d<sub>2</sub>** with KOD ( $0.32 \text{ s}^{-1}$ )<sup>20</sup> is further indication that the simulation gives reasonable rate constants.

**(3) Reactions of 3-d<sub>2</sub> with KOH in 50% MeCN–50% H<sub>2</sub>O:** These reactions did not provide interpretable results for two reasons. (a) Because of the slowness of the dedeuteration ( $k_{1,\text{D}}^{\text{OH}}$  is about 7-fold smaller than  $k_{1,\text{H}}^{\text{OH}} = k_{1,\text{H}}^{\text{OH}}$ , see Table 3) which is not offset by a reduced reprotonation of **3-d<sup>-</sup>**, the buildup of **3-d<sup>-</sup>** at the low end of the OH<sup>-</sup> concentration range is minimal, which results in absorbance changes that are too small for accurate kinetic data. (b) At higher OH<sup>-</sup> concentrations, the separation between  $k_{\text{obsd}}^{\text{I}}$  and  $k_{\text{obsd}}^{\text{II}}$  becomes too small for a reliable determination of  $k_{\text{obsd}}^{\text{I}}$ . Hence no data are reported for these experiments.

**Discussion**

**Kinetic and Thermodynamic Acidity of 3.** Table 1 reports rate constants for proton transfer and  $\text{p}K_{\text{a}}^{\text{CH}}$  values for **3** along with the corresponding parameters for **2a** and **6**. Compound **3** is seen to be substantially less acidic than **2a** or **6**. For example,  $\text{p}K_{\text{a}}^{\text{CH}}(\mathbf{3}) - \text{p}K_{\text{a}}^{\text{CH}}(\mathbf{2a}) = 1.97$  or, after statistical correction,  $\text{p}K_{\text{a}}^{\text{CH}}(\mathbf{3}) - \text{p}K_{\text{a}}^{\text{CH}}(\mathbf{2a}) = 1.79$ . This is consistent with the expectation that the resonance stabilization that arises from the contribution of the resonance structure **1<sup>±</sup>**, or **3<sup>±</sup>** for the specific case at hand, is particularly effective for this carbene complex. As mentioned in the Introduction, an exceptionally strong



contribution of **3<sup>±</sup>** to the resonance hybrid is indicated by <sup>53</sup>Cr NMR data. According to Hegedus et al.,<sup>11</sup> this must be the result of the oxygen being locked into a position for better  $\pi$ -overlap with the carbene carbon by virtue of the cyclic structure of **3<sup>±</sup>**.<sup>24</sup>

Our results contrast with Casey's<sup>3,4</sup> reports that in THF the acidities of **2a** and **3** are approximately the same. These acidities were measured by determining the equilibrium constants of the reactions of the PPN<sup>+</sup> salt<sup>5</sup> of the 4-cyanophenoxide ion with **2a** and **3**, respectively. We do not have a satisfactory explanation for the discrepancy between Casey's results and ours except to note that ion pairing in THF must be severe, which could lead to misleading results in that solvent if, e.g., the tightness of the ion pair between **2a<sup>-</sup>** and PPN<sup>+</sup> was different from that between **3<sup>-</sup>** and PPN<sup>+</sup>. Differences in ion pairing constants for a variety of ion pairs between **1<sup>-</sup>** and tetramethylguanidinium ion have been noticed even in acetonitrile solutions.<sup>25</sup> The effect of changing the identity of one of the ions in ion pairs in THF is also seen in the dramatic effect of replacing the PPN<sup>+</sup> by the Li<sup>+</sup> salt of 4-cyanophenoxide ion.<sup>26</sup>

With respect to proton transfer rates,<sup>27</sup> the number of bases amenable to study was much more limited than with **2a** or **6** because the high pK<sub>a</sub> of **3** leads to rates for the reprotonation of **3<sup>-</sup>** that, with most buffer acids, are too high for the stopped-flow technique. The only two bases that allowed kinetic measurements were OH<sup>-</sup> and piperidine. The results show that for **3** there is a decrease in the deprotonation rate constants ( $k_1^{\text{OH}}$  and  $k_1^{\text{Pip}}$ ) and an increase in the reprotonation rate constants ( $k_{-1}^{\text{H}_2\text{O}}$  and  $k_{-1}^{\text{PipH}^+}$ ) compared to **2a**, both of which contribute about equally to the higher pK<sub>a</sub> of **3**. This suggests

(24) A referee suggested that the increase in pK<sub>a</sub> is too large to be explained entirely by the extra stabilization of **3<sup>±</sup>** resulting from the ring structure of **3**. This is because the entropy difference between **2a** and **3** that arises from the freezing of one rotamer in the acyclic complex may not amount to more than about 4.5 gibbs/mol or the equivalent of about one pK unit. A contributing factor to the enhanced stability of **3<sup>±</sup>** compared to that of the corresponding resonance structure of **2a** (**1<sup>±</sup>** with R = CH<sub>3</sub> and R' = R'' = H) may be the stronger polarizability and hence increased electron donating effect of the alkyl chain attached to the oxygen in **3** compared to that of the methyl group attached to the oxygen in **2a**. This notion is supported by the fact that **2b** is less acidic than **2a** by about 0.5 pK units<sup>1</sup> as discussed in more detail below.

(25) Bernasconi, C. F.; Leyes, A. E.; Wulff, W. D. To be submitted for publication.

(26) Anderson, R. L. Ph.D. Thesis, University of Wisconsin, 1974; cited in ref 6.

(27) Casey and Brunsvold<sup>4</sup> were the first to measure deprotonation rates from **3** by studying the OD<sup>-</sup>-catalyzed  $\alpha$ -hydrogen exchange in **3** and its 5-methyl derivative in acetone/D<sub>2</sub>O solutions (3.6:1.0 by volume). For **3** they reported a  $k_{1,\text{H}}^{\text{OD}}$  value of 3.07 M<sup>-1</sup> s<sup>-1</sup> at 38 °C, which is 52-fold lower than our value in 50% MeCN–50% D<sub>2</sub>O (160 M<sup>-1</sup> s<sup>-1</sup>) at 25 °C. In view of the higher temperature and the fact that OD<sup>-</sup> is probably more basic in their acetone/D<sub>2</sub>O solution than in our solvent whereas the acidity of **3** is not expected to be greatly different in the two solvents, the true discrepancy between Casey's and our  $k_{1,\text{H}}^{\text{OD}}$  rate constant is likely to be even larger than a factor of 52. The reason for the discrepancy is a faulty data analysis by Casey and Brunsvold. In a typical experiment they used a 1.16 × 10<sup>-3</sup> M NaOD solution to which enough **3** was added to give a nominal [3] of 0.42 M. They then determined a first-order rate constant,  $k_{\text{obsd}} = 3.88 \times 10^{-3}$  s<sup>-1</sup>, by monitoring the decay of the CH<sub>2</sub> signal by <sup>1</sup>H NMR and calculated the second-order rate constant as  $k_{1,\text{H}}^{\text{OD}} = k_{\text{obsd}}/[\text{NaOD}]_0$ , with [NaOD]<sub>0</sub> being the base concentration before adding **3**. Since the large excess of **3** must have consumed most of the base, the actual equilibrium concentration of NaOD was of course much smaller than 1.16 × 10<sup>-3</sup> M. It is this equilibrium concentration that should be used in calculating the second-order rate constant, but this concentration is unknown in the absence of a pK<sub>a</sub> in that solvent.

that the intrinsic rate constant<sup>28</sup> ( $k_o^{\text{OH}}$ ,  $k_o^{\text{R}_2\text{NH}}$ ) for **3** and **2a** should be comparable. Such intrinsic rate constants can be estimated as follows. For deprotonation by OH<sup>-</sup>,  $\log k_o^{\text{OH}} \approx \log k_1^{\text{OH}} - 0.5 \log K_1^{\text{OH}}$ ,<sup>29</sup> for secondary cyclic amines  $\log k_o^{\text{R}_2\text{NH}} = \log(k_1^{\text{Pip}}/q) - 0.62(\Delta pK_a + \log p/q)$ ,<sup>31</sup> with 0.62 being the Brønsted  $\beta$  value for the deprotonation of **2a** by secondary alicyclic amines.<sup>10</sup> The  $\log k_o^{\text{OH}}$  and  $\log k_o^{\text{R}_2\text{NH}}$  values are included in Table 1. Within experimental error,  $\log k_o^{\text{OH}}$  and  $\log k_o^{\text{R}_2\text{NH}}$  for **3** are the same as for **2a**.

As discussed in more detail elsewhere,<sup>10,32</sup>  $\log k_o^{\text{R}_2\text{NH}}$  values in the order of 3.5 fall within the mid to low range of intrinsic rate constants for proton transfers from carbon acids. Since it is well-established that there exists an approximate inverse relationship between  $\log k_o$  for proton transfer from carbon acids and the degree of resonance stabilization of the carbanion,<sup>32,33</sup> our results confirm that **2a<sup>-</sup>** and **3<sup>-</sup>** must benefit from a substantial degree of resonance.

The observation that the  $k_o^{\text{OH}}$  and  $k_o^{\text{R}_2\text{NH}}$  values for **3** are about the same as for **2a** contrasts with our earlier findings<sup>10</sup> that for **6**  $k_o^{\text{OH}}$  is about 1.40 log units and  $k_o^{\text{R}_2\text{NH}}$  about 1.70 log units lower than for **2a** (Table 1). The lower intrinsic rate constants for **6** are mainly the result of the additional resonance stabilization of the anion by the phenyl group,<sup>34</sup> a stabilization that increases the acidity of **6** by 2.1 pK<sub>a</sub> units over that of **2a**.

Since the lower acidity of **3** relative to **2a** is also a resonance effect (**3<sup>±</sup>**), it is perhaps surprising that this extra resonance does not result in the kind of reduction in the intrinsic rate constants seen for the effect of the extra resonance in the anion of **6**. In order to understand this apparent inconsistency one needs to recall the reasons why resonance stabilization of products or reactants reduces intrinsic rate constants of reactions. The main reason is that the resonance effect at the transition state is typically disproportionately small, i.e., the development of product resonance lags behind bond changes (e.g., proton transfer) or the loss of reactant resonance is ahead of bond changes.<sup>32,33</sup> In the deprotonation of **3**, the expected reduction in the intrinsic rate by early loss of the extra resonance (**3<sup>±</sup>**) is apparently offset by an equivalent intrinsic rate enhancing factor. This factor may be attributed to preorganization of the (CO)<sub>5</sub>Cr moiety toward its structure and charge distribution in the anion **3<sup>-</sup>**. This preorganization has the effect of avoiding some of the intrinsic rate lowering lag in the charge delocalization into the (CO)<sub>5</sub>Cr moiety.

A similar situation exists in the comparison between **2a** and **2b**. The pK<sub>a</sub><sup>CH</sup> of **2b** (12.98)<sup>1</sup> is 0.48 units higher than that of **2a** (12.50), which has been attributed to a stronger electron

(28) For a reaction with a forward rate constant  $k_1$  and a reverse rate constant  $k_{-1}$ , the intrinsic rate constant,  $k_o$ , is defined as  $k_o = k_1 = k_{-1}$  when the equilibrium constant  $K_1 = 1$ . In proton transfers, statistical factors are usually taken into account (see footnote 31).

(29) This is equivalent to applying the simplest version of the Marcus equation;<sup>30</sup> the  $k_1^{\text{OH}}$  and pK<sub>a</sub><sup>CH</sup> values used are statistically corrected for the number of protons in **3** and **2a**.

(30) Marcus, R. A. J. *Chem. Phys.* **1965**, *43*, 679.

(31) This equation is based on determining  $\log k_o^{\text{R}_2\text{NH}}$  from a linear Brønsted-type plot of  $\log(k_1^{\text{R}_2\text{NH}}/q)$  vs  $\Delta pK_a + \log(p/q)$  by interpolation or extrapolation of the Brønsted line of slope  $\beta$  to  $\Delta pK_a + \log(p/q) = 0$ ;<sup>32,33</sup>  $k_1^{\text{R}_2\text{NH}}$  are rate constants for deprotonation of the carbon acid by a series of amines,  $\Delta pK_a$  is defined as  $pK_a^{\text{CH}} - pK_a^{\text{R}_2\text{NH}_2^+}$ ,  $p$  is the number of equivalent protons on R<sub>2</sub>NH<sub>2</sub><sup>+</sup>, and  $q$  is the number of equivalent basic sites on R<sub>2</sub>NH<sub>2</sub><sup>+</sup>; the  $k_1^{\text{Pip}}$  and pK<sub>a</sub><sup>CH</sup> values used are statistically corrected for the number of protons in **3** and **2a**.

(32) Bernasconi, C. F. *Adv. Phys. Org. Chem.* **1992**, *27*, 119.

(33) (a) Bernasconi, C. F. *Acc. Chem. Res.* **1987**, *20*, 301. (b) Bernasconi, C. F. *Acc. Chem. Res.* **1992**, *25*, 9.

(34) Increased steric hindrance, especially with the bulky piperidine, probably contributes somewhat to the lowering of the intrinsic rate constants for **6**.<sup>10</sup>

**Table 4.** Primary Kinetic Isotope Effects for Proton Transfer in Reactions of Fischer Carbene Complexes in 50% MeCN–50% Water at 25 °C

reaction	$pK_a^{CH} - pK_a^{BH}$ <sup>d</sup>	$k_H^B/k_D^B$ <sup>g</sup>	ref
<b>3</b> + OH <sup>-</sup>	2.17 <sup>e</sup>	7.20	this work
<b>2a</b> <sup>b</sup> + OH <sup>-</sup>	4.14 <sup>e</sup>	2.76	10
<b>6</b> <sup>c</sup> + OH <sup>-</sup>	6.24 <sup>e</sup>	2.53	10
<b>6</b> <sup>c</sup> + piperidine <sup>f</sup>	-0.61 <sup>f</sup>	5.51	10

<sup>a</sup>  $pK_a^{CH} = 14.47$ . <sup>b</sup>  $pK_a^{CH} = 12.50$ . <sup>c</sup>  $pK_a^{CH} = 10.40$ . <sup>d</sup> BH = H<sub>2</sub>O or piperidinium ion. <sup>e</sup>  $pK_a^{BH} = pK_a^{H_2O} = pK_w + \log[H_2O] = 16.64$ . <sup>f</sup>  $pK_a^{BH} = 11.01$ . <sup>g</sup>  $k_{1,H}^{OH}/k_{1,D}^{OH}$  or  $k_{1,H}^{Pip}/k_{1,D}^{Pip}$ .

donating effect of the ethyl compared to the methyl group, leading to enhanced  $\pi$ -donation (**1**<sup>±</sup>) in **2b** compared to **2a**.<sup>35</sup> Yet the  $\log k_o^{OH}$  values for deprotonation are the same within experimental error.<sup>1</sup>

**Kinetic Isotope Effects.** Primary kinetic isotope effects on the deprotonation of carbon acids by OH<sup>-</sup> are easily measured by comparing the rate constant of dedeuteration of the C–D acid ( $k_{1,D}^{OH}$ ) with that for deprotonation of the C–H acid ( $k_{1,H}^{OH} = k_{1,H}^{OH}$ ), provided the following two conditions are met: (1) The acidity of the carbon acid must be high enough so that the reaction can be conducted in a way that the deprotonation or dedeuteration is virtually irreversible; this scenario avoids complications from reprotonation of the carbanion of the C–D acid by H<sub>2</sub>O. (2) Subsequent reactions, such as hydrolysis in our case, must be slow enough as not to interfere significantly with the measurement of the proton and/or deuteron transfer. Both conditions were met in the reactions of **2a** and **6** with OH<sup>-</sup>,<sup>10</sup> but this is not the case for the reaction of **3** with OH<sup>-</sup>, as explained in the Results section. Hence no meaningful data were obtained from the reaction of **3-d**<sub>2</sub> with KOH.

In the reaction of **3** with KOD in 50% MeCN–50% D<sub>2</sub>O the opposite situation prevails. First, deprotonation is faster than in the reaction of **3** with KOH, due to the higher reactivity of OD<sup>-</sup> compared to OH<sup>-</sup>.<sup>37,38</sup> Second, capture of **3**<sup>-</sup> by D<sub>2</sub>O is slower than capture by H<sub>2</sub>O. Both of these effects contribute to make the conversion of **3** to **3**<sup>-</sup> more complete than in the KOH/MeCN/H<sub>2</sub>O system, and in fact, generation of **3**<sup>-</sup> “overshoots” as can be seen by subsequent depletion of **3**<sup>-</sup> in favor of **3-d** and **3-d**<sub>2</sub> (second kinetic process in Figure 4, see Scheme 1). It is these experiments, in conjunction with those of the reaction of **3-d**<sub>2</sub> in 50% MeCN–50% D<sub>2</sub>O, which provided the rate constants for the various substrate/solvent isotopic combinations summarized in Table 3.

The isotope effect results, summarized in Table 4, show that the deprotonation of **3** by OH<sup>-</sup> is subject to a substantial primary kinetic isotope effect ( $k_{1,H}^{OH}/k_{1,D}^{OH} \approx 7.2$ ), and so is the reprotonation of **3**<sup>-</sup> by D<sub>2</sub>O ( $k_{-1,H}^{H_2O}/k_{-1,H}^{D_2O} \approx 10.5$ ). The isotope effect for deprotonation of **3** by OH<sup>-</sup> is significantly larger than that for deprotonation of **2a** and **6** (Table 4). The extent by which the isotope effect for **3** exceeds those for **2a** and **6** is perhaps surprising, but the *direction* of the change is that expected based on the Westheimer model<sup>39</sup> for primary kinetic isotope effects. This is seen by considering the  $pK_a$  difference between proton

(35) The stronger electron donating effect is probably mainly the result of the greater polarizability of the ethyl group due to its larger size.<sup>36</sup> See also ref 24.

(36) Hine, J. *Structural Effects on Equilibria in Organic Chemistry*; Wiley-Interscience: New York, 1975; p 151.

(37) Laughton, P. M.; Robertson, R. E. In *Solute–Solvent Interactions*; Coetzee, J. F., Ritchie, C. D., Eds.; Dekker: New York, 1969; p 399.

(38) Casamassina, T. E.; Huskey, W. P. *J. Am. Chem. Soc.* **1993**, *115*, 14.

(39) (a) Westheimer, F. H. *Chem. Rev.* **1961**, *61*, 265. (b) More O’Ferrall, R. A. In *Proton Transfer Reactions*; Caldin, E., Gold, V., Eds.; Wiley & Sons: New York, 1975; p 201.

donor and acceptor which is smaller for the reaction of **3** with OH<sup>-</sup> than for the reactions of **2a** or **6** with OH<sup>-</sup>, suggesting a more symmetrical transition state and hence a larger isotope effect. The relatively large isotope effect for the deprotonation of **6** by piperidine (Table 4) for which the  $pK_a$  difference is small also fits into the observed pattern.

## Conclusions

(1) Compound **3** is less acidic than its acyclic analog **2a** by approximately 2  $pK_a$  units. This reduced acidity is attributed to enhanced stabilization of **3** by  $\pi$ -donation from the oxygen (**3**<sup>±</sup>) as suggested by <sup>53</sup>Cr NMR data. The extra stabilization is believed to be mainly a consequence of the cyclic structure which locks the oxygen into a position for better  $\pi$ -overlap. This notion is supported by a comparison of the hydrolysis rate constants of **3**, **2a**, and **6**.<sup>14</sup> A possible additional factor stabilizing **3** may be the greater polarizability and hence stronger electron donating ability of the alkyl group attached to the oxygen.<sup>24</sup>

(2) The lower acidity of **3** compared to **2a** is the combined result of lower deprotonation rate constants ( $k_1^{OH}$ ,  $k_1^B$ ) and higher reprotonation rate constants ( $k_{-1}^{H_2O}$ ,  $k_{-1}^{BH}$ ) for **3**, but the *intrinsic* rate constants for proton transfer ( $k_o^{OH}$ ,  $k_o^{R_2NH}$ ) are approximately the same for the two carbene complexes. The anticipated lowering of  $k_o^{OH}$  and  $k_o^{R_2NH}$  for **3** because of the resonance effect in **3** is apparently offset by an equivalent intrinsic rate enhancement that may be attributed to preorganization of the (CO)<sub>5</sub>Cr moiety toward its structure and charge distribution in **3**<sup>-</sup>.

(3) The primary kinetic isotope effect on the deprotonation of **3** by OH<sup>-</sup> is larger than for the same reaction of **2a**, consistent with the Westheimer model for a more symmetrical transition state.

(4) The complex kinetic behavior exhibited for the reaction of **3** with KOD in 50% MeCN–50% D<sub>2</sub>O is a consequence of the high  $pK_a^{CH}$  of **3**, which favors the un-ionized form under the reaction conditions. After deprotonation of **3** by OD<sup>-</sup>, **3**<sup>-</sup> is trapped by deuteron transfer from D<sub>2</sub>O. Hydrolysis is sufficiently slow that the concentration of **3-d** and **3-d**<sub>2</sub> increases temporarily before hydrolysis sets in.

## Experimental Section

**Materials.** 2-(Oxacyclopentylidene)pentacarbonylchromium(0) (**3**), a gift from Professor Hegedus, was recrystallized from dry pentane before use, mp 63.5–65.0 °C (lit. mp 63.5–65.0 °C).<sup>40</sup> **3-d**<sub>2</sub> was prepared by dissolving known amounts of **3** in 1.0 mL of 70% CD<sub>3</sub>CN–30% D<sub>2</sub>O in the presence of catalytic amounts of NaOD (<0.005 M). H/D exchange was monitored by <sup>1</sup>H NMR until no residual signal for the acidic protons of **3** at 3.6 ppm was observed. The resulting **3-d**<sub>2</sub> was not isolated, i.e., the NMR solutions were directly used for the kinetic experiments. (Methoxymethylcarbene)pentacarbonylchromium(0) (**2a**) was available from a previous study.<sup>12</sup> Piperidine was refluxed over sodium for at least 5 h in an argon atmosphere and then fractionally distilled. HCl and KOH solutions were prepared by diluting prepackaged stock solutions (Baker Analytical). Acetonitrile was purchased from Fisher Scientific and used as received. Water was obtained from a Millipore water purification system. CD<sub>3</sub>CN, D<sub>2</sub>O, and DCl were used as received.

**Solutions and pH Measurements.** All kinetic experiments were conducted in 50% CH<sub>3</sub>CN–50% H<sub>2</sub>O (v/v) or 50% CH<sub>3</sub>CN–50% D<sub>2</sub>O (v/v) solutions at 25 °C,  $\mu = 0.1$  M (KCl). All pH measurements were done with an Orion 611 pH meter equipped with a glass electrode and a “SureFlow” (Corning) reference electrode and calibrated with standard aqueous buffers. Actual pH values were calculated by adding 0.18 to

(40) Casey, C. P.; Anderson, R. L. *J. Organomet. Chem.* **1974**, *73*, C28.

the measured pH, according to Allen et al.<sup>41</sup> The pH of reaction solutions for stopped-flow experiments was adjusted in mock-mixing experiments which mimicked the stopped-flow runs. The pK<sub>a</sub> value of piperidine was known from a previous study.<sup>10</sup>

**Kinetics and Spectra.** Typical substrate concentrations were  $(5-10) \times 10^{-5}$  M. Rates were measured in an Applied Photophysics DX.17MV stopped-flow apparatus (fast rates) and in a Perkin-Elmer Lambda 2 or Hewlett-Packard 8452A diode array UV-vis spectrophotometer (slow rates). Kinetics were followed by monitoring the disappearance of the substrate at 364 nm. Rate constants ( $k_{\text{obsd}}$ ) were obtained by computer fit programs (Applied Photophysics and Enzfitter<sup>42</sup>). The time-dependent spectra shown in Figure 1 were taken on a Durrum-Gibson stopped-flow apparatus equipped with an OLIS RSM 1000 rapid scan spectrophotometer.

**Computer Simulations.** Kinetic traces of the reaction of **3** with KOD in 50% MeCN-50% D<sub>2</sub>O were simulated on a PC with use of the simulation program KINETICS.<sup>43</sup> The general procedure was to input the chemical equation along with the known/estimated microscopic rate constants and initial reactant concentrations. Numerical integration over the desired time period results in a matrix containing concentrations of each of the species as a function of time. Kinetic

traces at 364 nm were generated from concentrations and extinction coefficients of each of the absorbing species, and simulated kinetic profiles were curve fitted and rate constants determined. Extinction coefficients (in units of M<sup>-1</sup> cm<sup>-1</sup>) were determined as follows:  $\epsilon(\mathbf{3}) = 7.4 \times 10^3$ ,  $\epsilon(\mathbf{3-d}_2) = 7.6 \times 10^3$ ,  $\epsilon(\text{products}) = 1.9 \times 10^3$ ,  $\epsilon(\mathbf{3}^-) = (1.36 \pm 0.24) \times 10^3$ , and  $\epsilon(\mathbf{3-d}^-) \approx 1.2 \times 10^3$ . The latter two extinction coefficients were estimated from the kinetic traces for proton transfer which had the shape of an exponential decrease followed by a sloping infinity. Extrapolation of the sloping part of the trace to zero time was taken as the absorbance of the system in a hypothetical equilibrium situation between **3** and **3**<sup>-</sup> (or **3-d**<sub>2</sub> and **3-d**<sup>-</sup>). Observed absorbance was thus given by  $\text{OD} = \epsilon(\mathbf{3})[\mathbf{3}] + \epsilon(\mathbf{3}^-)[\mathbf{3}^-]$ .  $\epsilon(\mathbf{3}^-)$  was obtained from the above equation with use of initial substrate and KOH concentrations,  $K_1^{\text{OH}}$  and  $\epsilon(\mathbf{3})$ . This estimation was carried out at various concentrations of [KOH] or [KOD] to afford average  $\epsilon(\mathbf{3}^-)$  and  $\epsilon(\mathbf{3-d}^-)$  values.

**Acknowledgment.** This work has been supported by Grant No. CHE-9307659 from the National Science Foundation and by the donors of the Petroleum Research Fund, administered by the American Chemical Society, Grant No. 30444-AC4. We also thank Professor Louis Hegedus for providing us with (2-oxacyclopentylidene)pentacarbonylchromium(0).

JA964069B

(41) Allen, A. D.; Tidwell, T. T. *J. Am. Chem. Soc.* **1987**, *109*, 2774.

(42) Program by R. J. Leatherbarrow, distributed by BIOSOFT, 22 Hills Road, Cambridge, CB2 1JP, United Kingdom.

(43) Program by K. J. Tupper, distributed by ARSoftware Co., 8201 Corporate Dr., Suite 1110, Landover, MD 20785.